Available online at www.sciencedirect.com
SCIENCE DIRECT
Polymer 46 (2005) 955–963
polymer
www.elsevier.com/locate/polymer

Studies of hydrodynamic properties for characterizing star-shaped poly(ethylene-*co*-propylene)

Hsuan-Ming Huang, I-Chun Liu, Raymond Chien-Chao Tsiang*

Department of Chemical Engineering, National Chung Cheng University, Chiayi, Taiwan, ROC

Received 28 July 2004; received in revised form 30 September 2004; accepted 30 November 2004
Available online 13 December 2004

Abstract

Linear and star-shaped polyisoprene were synthesized and hydrogenated to form the targeted poly(ethylene-*co*-propylene) copolymers, $(EP)_{lin}$ and $(EP)_{star}$. Hydrodynamic properties of the polymers in THF at 40 °C have been studied by gel permeation chromatography, using multiple-angle laser light scattering and differential refractive index detectors.

The radius of gyration R_g of $(EP)_{star}$ was found proportional to the molecular weight to a power of 0.34 corroborating a globular architecture and the R_g of $(EP)_{lin}$ to a power of 0.60 indicating a random coil conformation in a good solvent. The intrinsic viscosity $[\eta]$ of $(EP)_{lin}$ was much higher than that of $(EP)_{star}$ due to the compact globular structure of star molecules. While the $[\eta]$ of $(EP)_{lin}$ increased with an increase in the molecular weight, the molecular weight had little effect on the $[\eta]$ of $(EP)_{star}$ as long as the arm length was fixed. Based on the measured R_g and $[\eta]$, the coefficient q for the scaling law, the Mark–Houwink constant α, and the hydrodynamic radius R_e have been calculated. The hydrodynamic radius R_e was approximately 0.78 times of R_g for $(EP)_{lin}$ and was nearly identical to R_g for $(EP)_{star}$. The value of R_e/R_g appeared to be independent of the molecular weight for both linear and star polymers and was almost equal to those of polystyrene and polyisoprene in good solvents.

Keywords: Star polymer; Radius of gyration; Hydrodynamic radius

1. Introduction

Solution properties of block copolymers have been studied extensively in the past decade [1–4]. Most of the theoretical and experimental work was devoted to linear diblock and triblock copolymers. Studies of star-shaped block copolymers are very limited even though star-shaped homopolymers and miktoarm copolymers have been thoroughly investigated [5–11]. Typically, star-shaped polymers with a unique three-dimensional macromolecular architecture can be produced via an 'arms-first, core-last' method by reacting monofunctional polymeric arms with crosslinkable, core-forming co-monomers such as 1,3-diisopropenylbenzene and divinylbenzene [12–15]. The number of arms and the total molecular weight increases with the weight percent of core materials. Among various star-shaped copolymers, it is essential to study the poly(ethylene-*co*-propylene), $(EP)_{star}$ because a star-shaped poly(ethylene-*co*-propylene) copolymer can be used as a viscosity index improver in lubricants [16,17]. Generally speaking, a multiple-angle laser light scattering (MALLS) measurement is effective in providing the distribution of absolute molecular weight and detecting the aggregation behavior of polymer solutions in a wide range of polymer concentrations. In literatures, Tarazona et al. studied poly(alkoxy/aryloxy phosphazene) and used the MALLS to better understand the solution properties [18–20]. Ishizu et al. found that star-shaped poly[isoprene(I)-*b*-I/styrene(*S*)-*b*-S] molecules behaved not as hard spheres but as soft spheres which were penetrable near the edge to good solvents [21]. Therefore, in our work a gel permeation chromatograph hyphenated with a refractometric detector (RI) and a MALLS detector was used to measure hydrodynamic solution properties and understand how the molecular architecture affects those properties. Based on

* Corresponding author. Tel.: +886 5 242 8122; fax: +886 5 272 1206.
E-mail address: chmcct@ccu.edu.tw (R.C.-C. Tsiang).

0032-3861/$ - see front matter © 2004 Elsevier Ltd. All rights reserved.
doi:10.1016/j.polymer.2004.11.102

these measurements, information about the scaling law, $R_g = QM^q$ and the hydrodynamic dimensions of polymers could be obtained.

2. Experimental

2.1. Materials

Isoprene was purchased from Tokyo chemical Industry and pretreated under nitrogen with activated alumina (from Alcoa Co.) prior to its use. Cyclohexane was obtained from Taiwan Synthetic Rubber Corporation (TSRC) and was distilled and treated with activated alumina. Tetrahydrofuran (THF) was purchased from BDH and pretreated with activated alumina. *n*-Butyllithium (*n*-BuLi) was purchased from Merck as a 15 wt% solution in hexane. Divinylbenzene (DVB) was purchased from Tokyo Chemical Industry at 55% purity.

2.2. Synthesis of star-shaped polyisoprene, $(I)_{star}$

The synthesis of $(I)_{star}$ was accomplished via anionic polymerization in cyclohexane. The reaction scheme of $(I)_{star}$ is show in Scheme 1. To a 1 l pressure vessel under a slight nitrogen overpressure were added 550 ml of cyclohexane and 0.1 ml of THF (amounted to 200 ppm, to accelerate the polymerization). The vessel was then heated to 40 °C followed by the addition of *n*-BuLi solution.

Subsequently, isoprene monomer was charged to the reactor. The color turned to light yellow, indicating the presence of living polyisoprenyllithium anions. Thirty minutes later 2 ml of THF was charged to the vessel to facilitate the successive linking reaction. The vessel was heated to 60 °C. DVB at a desired [DVB]/[*n*-BuLi] ratio was then added to the living polymeric chains to form the desired $(I)_{star}$. The linking reaction was allowed to take place for 45 min before quenching with methanol and precipitating the final polymer in isopropanol. The precipitated sample was then oven-dried.

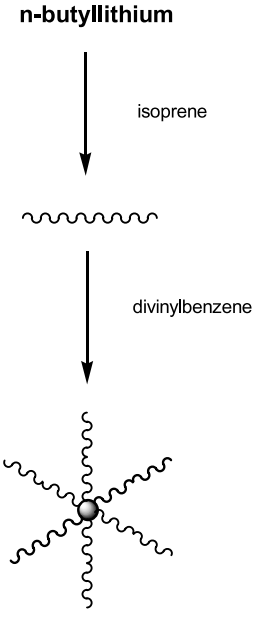

Scheme 1. Synthesis of $(I)_{star}$.

2.3. Hydrogenation of $(I)_{star}$

The hydrogenation reaction was conducted following well-established procedures using nickel octoate and triethylaluminum as the catalysts [22–24]. The hydrogenation reaction was carried out in a 2 l mechanically stirred autoclave (made by PPI, rated to 6000 psi) at 80 °C for 8 h. $(I)_{star}$, 330 g of a 7.3 wt% solution in cyclohexane was charged to the autoclave, followed by the premixed catalyst solution with a loading of 7000 ppm Ni at an Al/Ni molar ratio of 2.3. The hydrogen pressure was then kept constant at 3000 psi, with the reaction mixture saturated with the hydrogen. Samples of the reaction mixture were taken at fixed time intervals, and were repeatedly washed with dilute sulfuric acid to remove the residual catalyst. After adding Irganox 1076 as a stabilizer the hydrogenated copolymer was then precipitated in isopropanol and dried at 50 °C in a vacuum oven. This hydrogenated copolymer, $(EP)_{star}$, exhibited a structure consisting of 95% ethylene and propylene unit and 5% methyl butane unit, arising from the hydrogenated forms of various isomeric polyisoprene elements in the unhydrogenated $(I)_{star}$ [25] (see Scheme 2).

2.4. Analysis of $(EP)_{star}$

The molecular weight and molecular weight distribution of synthesized $(EP)_{star}$ were determined by Waters gel permeation chromatography (GPC) equipped with a Waters 410 differential refractive index (RI) detector and a multiple-angle laser light scattering (MALLS, miniDAWN model, Wyatt Technology Corporation) detector. The GPC was typically operated using three Waters Styragel columns (HR 3, HR 4 and HR 5) at a normal flow rate of 1 ml/min with a sample concentration of 0.1% at 40 °C in THF. The MALLS detector was equipped with a 20 mW semiconductor laser (690 nm). The molecular weight determination using MALLS necessitated the measuring of refractive index increment, d*n*/d*c* (specific refractive index increment). The d*n*/d*c* of the synthesized polymer, at the same wavelength of light as the MALLS, was measured by the

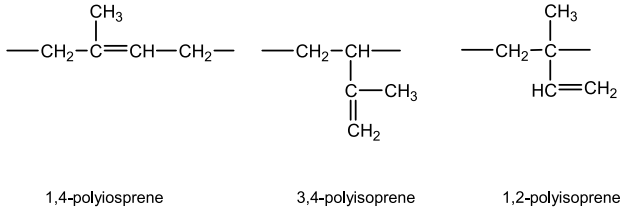

Scheme 2. Isomeric isoprene units in polyisoprene.

Wyatt/Optilab DSP interferometric refractometer. Our results indicated that the dn/dc of a $(EP)_{star}$ molecule did not vary with the arm length or the degree of branching. The dn/dc value determined for all $(I)_{star}$ samples synthesized in this work was $0.1027 \pm 1\%$. The hydrogenation reaction was confirmed by the disappearance of the double bond peaks of the trans-1,4, cis-1,4, vinyl-1,2 and 3,4 units in the FTIR spectrum (at 1663, 1644, 888 and 836 cm^{-1}, respectively) as shown in Fig. 1. A Shimadzu FTIR-8101M instrument with a liquid N_2 cooled MCT detector was used with a spectral resolution of 2 cm^{-1}. The samples were prepared as cast films on KBr plates. Flow times for solvent (THF) and polymer solutions at various concentrations were measured in Ubbelohde viscometer. Data were analyzed by aid of the equation

$$[\eta] = \frac{\eta - \eta_s}{\eta_s \rho}|_{\rho=0} \tag{1}$$

where $[\eta]$ is the intrinsic viscosity, η is solution viscosity, η_s is solvent viscosity, and ρ is the density of monomer units in the solution, respectively. For the solution of spheres of radius R_e Einstein derived

$$\eta = \eta_s(1 + 2.5\phi) \tag{2}$$

where ϕ is the volume fraction occupied by the spheres in the solution. If each sphere consists of N monomer units of mass m and their density is ρ, we have:

$$\phi = \frac{N_A \rho}{mN} \frac{4\pi}{3} R_e^3 = \frac{N_A \rho}{M_w} \frac{4\pi}{3} R_e^3 \tag{3}$$

From Eqs. (2) and (3), we get

$$[\eta] = 2.5 \frac{4\pi}{3} N_A \left(\frac{R_e^2}{M_w}\right)^{3/2} M_w^{1/2} \tag{4a}$$

which can be converted into

$$R_e = \left(\frac{3}{10\pi N_A}\right)^{1/3} ([\eta] M_w)^{1/3} \tag{4b}$$

where N_A is Avogadro number and M_w is the weight average molecular weight determined by MALLS. Hydrodynamic radius, R_e, was calculated from Eq. (4b) based on the measurement of intrinsic viscosity.

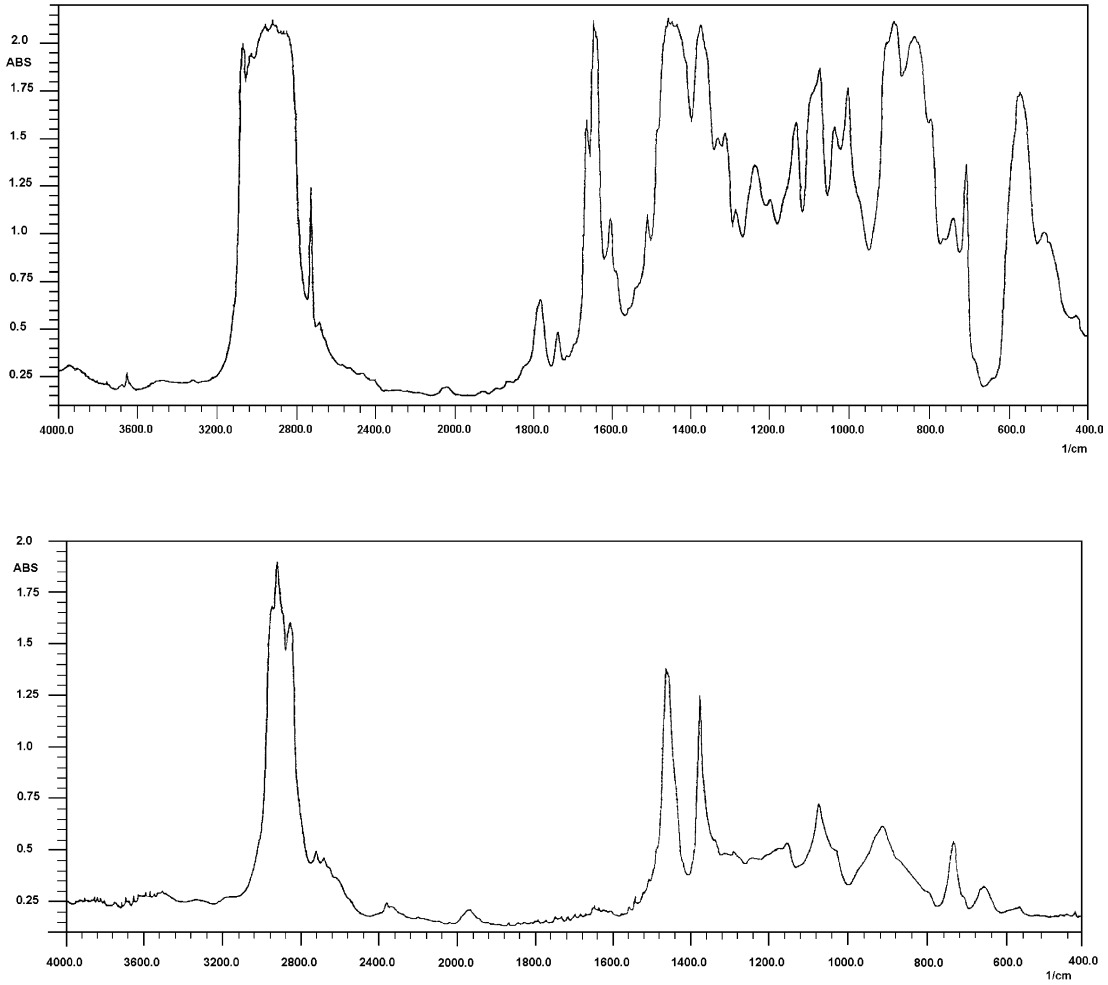

Fig. 1. FTIR spectra of the star molecule $(EP)_{star}$-2 before and after hydrogenation (top: before hydrogenation; bottom: after hydrogenation).

3. Results and discussion

The GPC-RI chromatograms of $(EP)_{star}$ are shown in Fig. 2. Detected by the RI detector, peak B at the higher elution volume corresponded to the unlinked linear chains $(EP)_{arm}$ and the peak A at the lower elution volume corresponded to the $(EP)_{star}$. However, the UV detector did not detect peak B because of the lack of benzyl groups of DVB in unlinked arms for characteristic UV absorption. The absence of peak B under the UV detector also indicated that all of the DVB were consumed in the core formation of $(EP)_{star}$. The linking efficiency of arms by DVB (i.e., the fraction of arms that have been linked into star molecules) was determined according to the GPC chromatogram of $(EP)_{star}$ based on the areas underneath the two peaks [17]. All characteristic data of $(EP)_{star}$ are summarized in Table 1. The linking efficiency was limited by the purity (55%) of DVB and the presence of DVB isomers (*p*-DVB linked less efficiently than *m*-DVB [26]), and the highest efficiency ever achieved was 83.6%. Generally, the molecular weights for $(EP)_{star}$ measured using the GPC-RI were much lower than their absolute values. This was attributed to the higher segmental density of star molecules in a solution than their linear counterparts [6], thus resulting in lower hydrodynamic volumes when compared at the same molecular weight. In contrast, the molecular weights for linear arms measured with the GPC-RI (calibrated with the linear polystyrene standards) were higher than their absolute values because poly(ethylene-*co*-propylene) had a larger hydrodynamic volume than polystyrene when compared at the same molecular weight.

In order to measure the absolute molecular weight of the $(EP)_{star}$ and the arms, the GPC–MALLS measurements were conducted. All the GPC–MALLS data of $(EP)_{star}$ are also summarized in Table 1. The absolute molecular weight of the $(EP)_{star}$ and its arms, were calculated from the intercepts on the ordinate of the Debye plot of the follow equation

$$\frac{KC}{R_\theta} \approx \frac{1}{M_w}\left[1 + \frac{16\pi^2}{3\lambda^2}\langle R_g^2\rangle \sin^2\left(\frac{\theta}{2}\right)\right] \quad \text{at low concentration} \tag{5}$$

where R_θ is the Rayleigh scattering intensity at the angle θ, M_w is the molecular weight, C is the concentration of polymer solution, $\langle R_g^2\rangle$ is the mean square radius of gyration, λ is the wavelength of the incident light in the solvent, K is an optical parameter that is a function of polymers. The degree of branching (i.e., the number of arms per star molecule), f, defined as the molecular weight ratio of star molecule to the arm, increased with an increase in the mole ratio of DVB to *n*-BuLi. However, the value of f determined from the absolute molecular weights (measured with GPC–MALLS) was generally 5–7 higher than that from GPC-RI molecular weights. Furthermore, to investigate the difference in solution properties between linear and star-shaped poly(ethylene-*co*-propylene), three linear $(EP)_{lin}$ were synthesized as model samples as shown in Table 2. These $(EP)_{lin}$ were synthesized to have molecular weights nearly identical to those $(EP)_{star}$. The Debye plots generated by

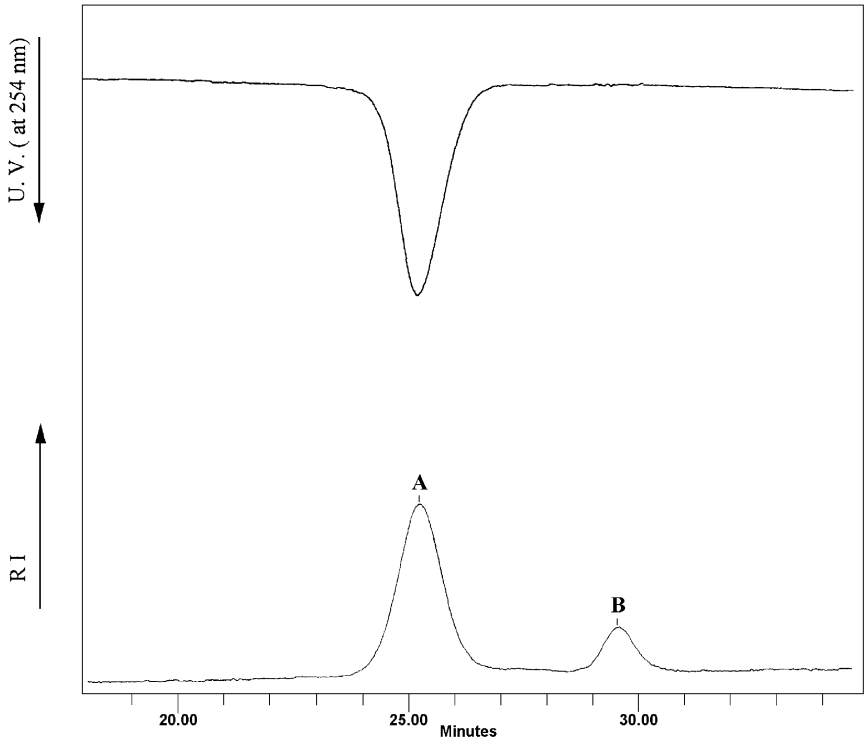

Fig. 2. GPC chromatograms of the formed star molecule $(EP)_{star}$-2: above: by UV detector; below: by RI detector (A, star molecule; B, linear arm).

Table 1
Molecular weight measurements for star-shaped $(EP)_{star}$

Polymer	R	$(M_w)_{arm}$	$(M_w)_{star}$	f	PDI	Linking eff.
GPC-RI measurements						
$(EP)_{star}$-1	3	2.81×10^4	29.63×10^4	10.5	1.25	82.3
$(EP)_{star}$-2	6	2.51×10^4	48.16×10^4	19.2	1.25	83.6
$(EP)_{star}$-3	9	2.61×10^4	60.52×10^4	23.3	1.19	82.2
GPC–MALLS measurements						
$(EP)_{star}$-1	3	2.25×10^4	33.96×10^4	15.1	1.21	81.2
$(EP)_{star}$-2	6	2.31×10^4	54.13×10^4	23.4	1.24	81.4
$(EP)_{star}$-3	9	2.09×10^4	64.37×10^4	30.8	1.20	82.5

R, molar ratio of DVB to *n*-butyllithium; f, degree of branching based on ($f=(M_w)_{star}/(M_w)_{arm}$).

MALLS instrument for $(EP)_{lin}$-2 and $(EP)_{star}$-2 shown in Figs. 3 and 4 indicate the accuracy of the absolute molecular weight measurements. The linking efficiency of arms by DVB was easily determined from the cumulative weight fraction versus the molecular weight plot in Fig. 5. For $(EP)_{star}$-2 there existed a discontinuous plateau under which was the weight fraction (18.6%) of unlinked arms and above which was the weight fraction (81.4%) of star molecules, i.e. the linking efficiency. This linking efficiency was in good agreement with that calculated based on the peak areas from GPC-RI analyses.

With the GPC–MALLS, the radius of gyration was measured from the angular dependence of the intensity of the scattered light. For the purpose of illustration, the root-mean-square radius of gyration (R_g) was measured versus the elution volume for $(EP)_{star}$-2 and $(EP)_{lin}$-2 as shown in Fig. 6. The R_g of $(EP)_{star}$-2 was markedly smaller than $(EP)_{lin}$-2 regardless of nearly identical molecular weights. The R_g of both $(EP)_{lin}$-2 and $(EP)_{star}$-2 decreased with the elution volume in accord with the separation mechanism of GPC. The light scattering signal was weak for low molecular weight species and, therefore, the accuracy of the radius of gyration measured in the region of high elution volumes (>20 ml) was poor.

Molecular architectures of the polymers in solution were investigated with the scaling law: $R_g=QM^q$ where q is a shape parameter. Generally, q has a value of 1/3 for globular polymers and 1/2 for random coil polymers at theta conditions [27]. For random coil polymers in good solvents, the value of q could increase up to 0.6 [28,29]. The log–log plots of the radius of gyration versus molecular weight for $(EP)_{lin}$-2 and $(EP)_{star}$-2 are shown in Fig. 7. Exclusive of the low-molecular-weight species (due to the inaccuracy of light scattering data), the linear regression analyses indicated that the q value for $(EP)_{star}$-2 was 0.34 ± 0.012 which corroborated the globular shape of the molecule. On the other hand, the q value for $(EP)_{lin}$-2 was 0.60 ± 0.007 indicating the random coil molecules in a good solvent. Assuming R_e was proportional to R_g (which has been corroborated later in the text), Eq. (4a) would enable us to calculate the constant α in the Mark–Houwink equation (i.e. $[\eta]=KM_w^{\alpha}$) for linear $(EP)_{lin}$ based on the empirical value of q parameter: For example, since $R_e\propto R_g\propto M_w^{0.6}$ for $(EP)_{lin}$-2

$$[\eta]\propto\left(\frac{R_e^2}{M_w}\right)^{3/2}M_w^{1/2}\propto M_w^{0.8} \tag{6}$$

the Mark–Houwink constant α for linear $(EP)_{lin}$-2 in THF at 40 °C is 0.8. Calculated values of q parameter and Mark–Houwink constant α for all $(EP)_{lin}$ are listed in Table 3. Because intrinsic viscosity reflects the chain conformation of the polymer in dilute solution, it was worthwhile to study the effect of the degree of branching on viscosity. As depicted in Table 4, for molecules with the same molecular weight the intrinsic viscosity of $(EP)_{lin}$ was much higher than $(EP)_{star}$ because the compact globular structure of star molecules made the hydrodynamic volume much smaller. Furthermore, for linear polymer $(EP)_{lin}$ the intrinsic viscosity increased with an increase in the molecular weight, but for star polymer $(EP)_{star}$ having a fixed arm length the molecular weight (or the degree of branching) had little effect on viscosity. It was conceivable that the intramolecular arm entanglement of the star molecules significantly thwarted the intermolecular chain entanglement. Similar observation that as long as the arm length is

Table 2
Molecular weight measurements for linear $(EP)_{lin}$

Polymer	$(M_w)^a$	$(M_w)^b$	PDI[a]
$(EP)_{lin}$-1	25.34×10^4	33.25×10^4	1.081
$(EP)_{lin}$-2	42.10×10^4	55.04×10^4	1.112
$(EP)_{lin}$-3	52.13×10^4	68.54×10^4	1.191

[a] (M_w), GPC–RI measurements.
[b] (M_w), GPC–MALLS measurements.

Table 3
q parameter and Mark–Houwink constant α for all sample

Sample no.	q	α
Linear		
$(EP)_{lin}$-1	0.59	0.77
$(EP)_{lin}$-2	0.60	0.80
$(EP)_{lin}$-3	0.59	0.77
Star		
$(EP)_{star}$-1	0.33	–
$(EP)_{star}$-2	0.34	–
$(EP)_{star}$-3	0.34	–

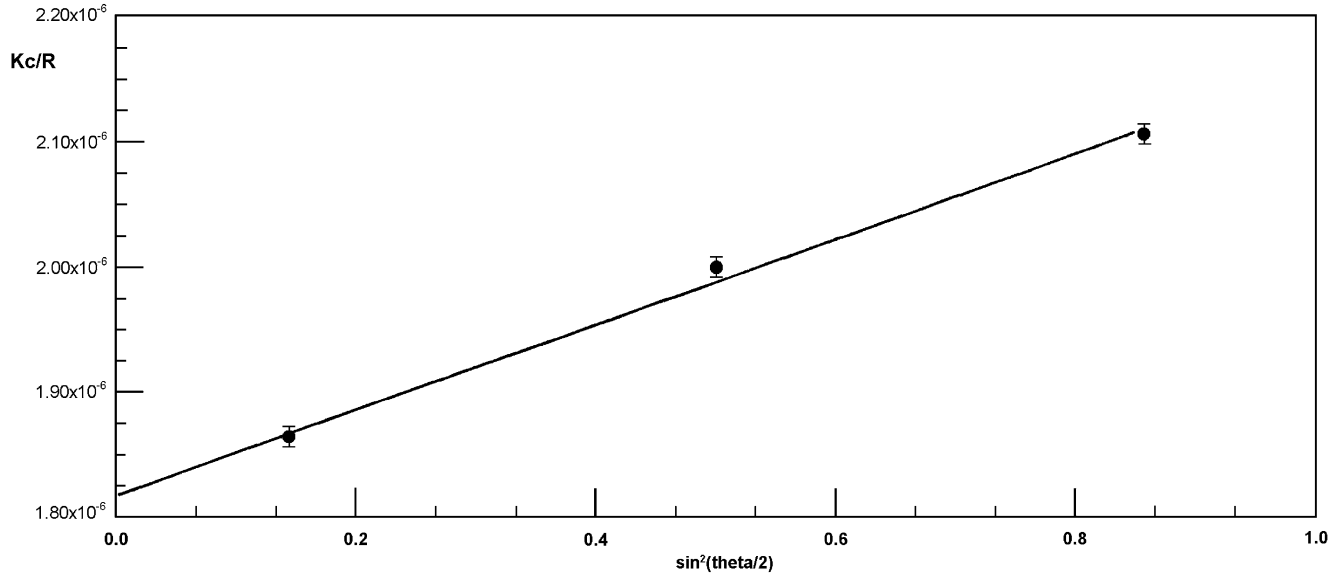

Fig. 3. The Debye plot generated by MALLS instrument for $(EP)_{lin}$-2.

Table 4
Intrinsic viscosity, hydrodynamic radius, radius of gyration and the value of R_e/R_g for all samples

Sample no.	$\eta_{intrinsic}$ (dl/g)	R_e (nm)	R_g (nm)	R_e/R_g
Linear				
$(EP)_{lin}$-1	1.240	18.1	23.1	0.78
$(EP)_{lin}$-2	1.354	22.7	29.4	0.77
$(EP)_{lin}$-3	1.541	26.7	34.8	0.77
Star				
$(EP)_{star}$-1	0.370	12.5	12.2	1.02(15.1)[a]
$(EP)_{star}$-2	0.357	14.5	14.1	1.03(23.4)
$(EP)_{star}$-3	0.398	15.9	15.2	1.05(30.8)

[a] Number in parenthesis indicates the degree of branching.

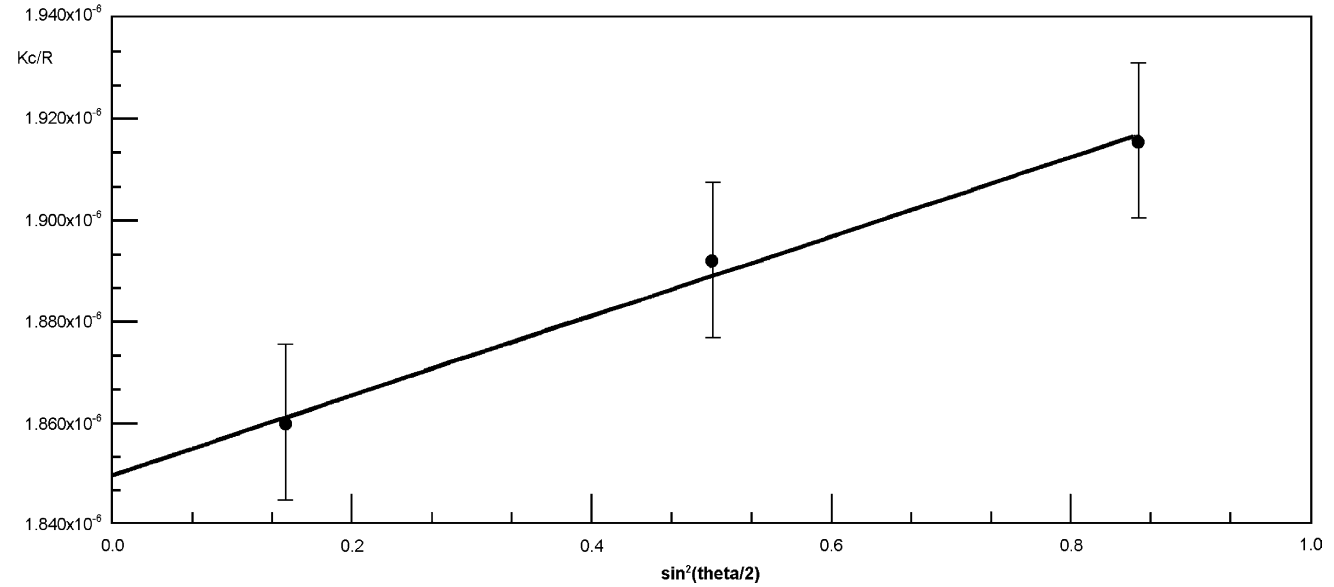

Fig. 4. The Debye plot generated by MALLS instrument for $(EP)_{star}$-2.

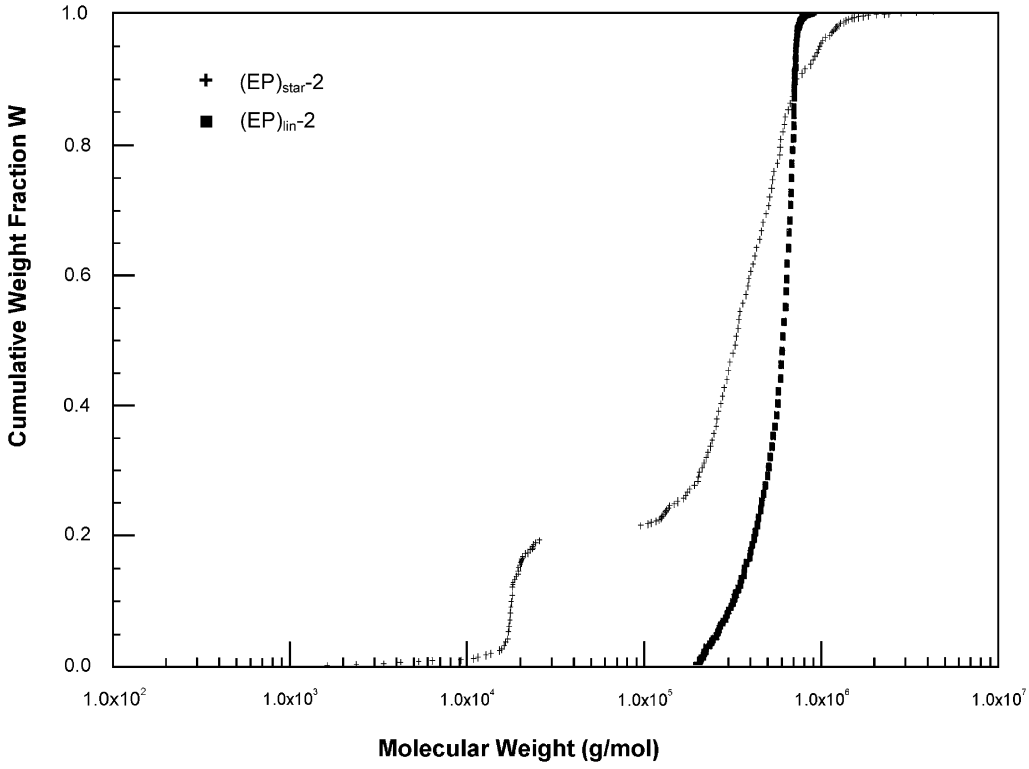

Fig. 5. The cumulative weight fraction versus logarithm of molecular weight made in $(EP)_{lin}$-2 and $(EP)_{star}$-2.

constant the intrinsic viscosity remains unchanged regardless of the number of arms has also been previously reported by us in other cases [16]. Based on the intrinsic viscosity data, the hydrodynamic radius R_e was calculated using Eq. (4b) and compared with the R_g. As shown in Table 4, while the R_e was approximately 0.78 times of R_g for $(EP)_{lin}$, the R_e was nearly identical to R_g for $(EP)_{star}$. The observation that R_e was nearly identical to R_g for star polymers in a good solvent agreed with previous report by others [30]. Besides, the value of R_e/R_g appeared to be independent of the molecular weight for both linear and star polymers. Comparisons of poly(ethylene-*co*-propylene) with other polymers in a good solvent are shown in Table 5. Theoretical predictions for unperturbed coils (in theta solvents), self-avoiding coils (in good solvents), and spheres are also listed in this table. The values of R_e/R_g for linear polystyrene, polyisoprene and poly(ethylene-*co*-propylene) in good solvents were in excellent agreement with each other and in reasonable agreement with the theory of self-avoiding coils. Therefore, it was suggested that the hydrodynamic penetration was similar in good solvents

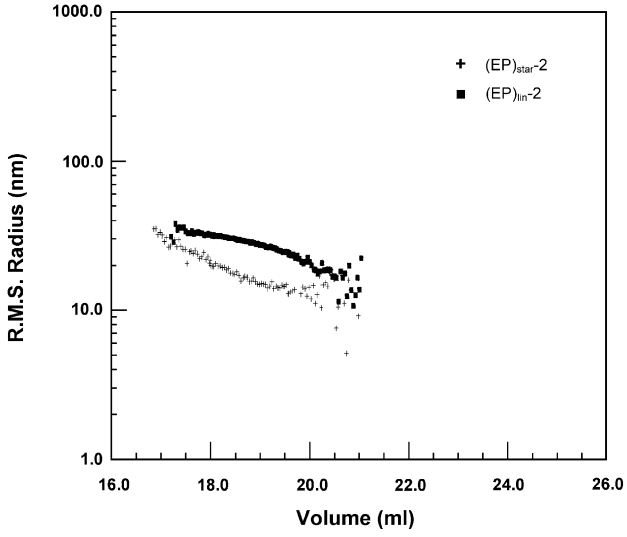

Fig. 6. The value of the root-mean-square radius of gyration R_g versus the elution volume made in $(EP)_{star}$-2 and $(EP)_{lin}$-2.

Table 5
Comparison of experimental and theoretical size ratios

Polymer	Solvent	R_e/R_g	Reference
Linear			
Polystyrene	Benzene	0.79	[32,33]
Polyisoprene	Cyclohexane	0.79	[31]
Poly(ethylene-*co*-propylene)	THF	0.78	This work
Unperturbed coils (theory)		1.00	[34,35]
Self-avoiding coils (theory)		0.72	[35]
Star			
Polystyrene	Benzene	1.13	[32]
Polyisoprene	Cyclohexane	1.05	[30]
Poly(ethylene-*co*-propylene)	THF	1.03	This work
Spheres (theory)		1.29	[30,36]

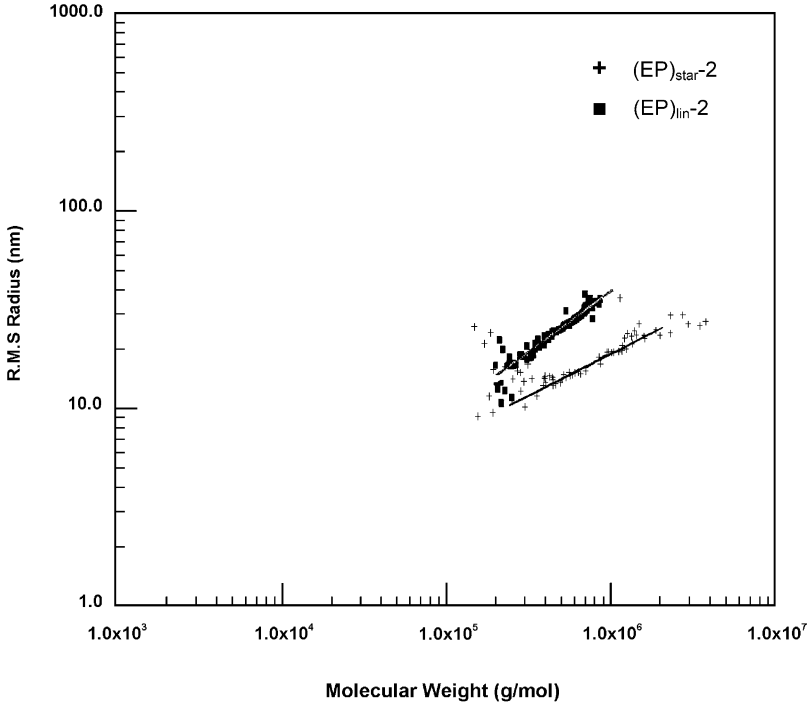

Fig. 7. The log–log plot of the radius of gyration versus molecular weight for $(EP)_{lin}$-2 and $(EP)_{star}$-2.

regardless of the chemical composition and the number of arms of the star polymers.

4. Conclusions

Linear and star-shaped poly(ethylene-*co*-propylene) copolymers, $(EP)_{star}$ and $(EP)_{lin}$, having the same molecular weights were synthesized to study the hydrodynamic properties. A maximum linking efficiency of 83.6% has been achieved during the synthesis of $(EP)_{star}$. GPC–MALLS is indispensable to the measurement of the absolute molecular weight. The R_g of $(EP)_{star}$ is markedly smaller than that of $(EP)_{lin}$ regardless of the identical molecular weights. The R_g of $(EP)_{star}$ is proportional to the molecular weight to a power of 0.34 corroborating a globular architecture and the R_g of $(EP)_{lin}$ to a power of 0.60 indicating a random coil conformation in a good solvent. The Mark–Houwink constant α for $(EP)_{lin}$ in THF at 40 °C was estimated as 0.80. The intrinsic viscosity of $(EP)_{lin}$ was much higher than $(EP)_{star}$ because the compact globular structure of star molecules made the hydrodynamic volume much smaller. Furthermore, while the intrinsic viscosity of $(EP)_{lin}$ increased with an increase in the molecular weight, the molecular weight (or the degree of branching) had little effect on the intrinsic viscosity of $(EP)_{star}$ as long as the arm length was fixed. The hydrodynamic radius R_e was approximately 0.78 times of R_g for $(EP)_{lin}$ and was nearly identical to R_g for $(EP)_{star}$. The value of R_e/R_g appeared to be independent of the molecular weight for both linear and star polymers and was almost equal to those of polystyrene and polyisoprene in good solvents. Thus, it was suggested that the hydrodynamic penetration was similar in good solvents regardless of the chemical composition and the number of arms of the star polymers.

References

[1] Tuzar Z, Kratochvil P. Adv Colloid Interface Sci 1976;6:201.
[2] Alexandridis P, Hatton TA. Colloid Surf A 1995;96:1.
[3] Laguna MTR, Tarazona MP. Polymer 2001;42:1751.
[4] Pezzin G, Lora S, Busulini L. Polym Bull 1981;5:543.
[5] Toporowski PM, Roovers J. Macromolecules 1978;11:365.
[6] Roovers J, Hadjichristidis N, Fetters LJ. Macromolecules 1983;16:214.
[7] Douglas JF, Roovers J, Freed KF. Macromolecules 1990;23:4168.
[8] Vlahos C, Tselikas Y, Hadjichristidis N, Roovers J, Rey A, Freire J. Macromolecules 1996;29:5599.
[9] Tsitsilianis C, Kouli O. Makromol Rapid Commun 1995;16:591.
[10] Tsitsilianis C, Papanagopoulos D, Lutz P. Polymer 1995;36:3745.
[11] Voulgaris D, Tsitsilianis C, Esselink FJ, Hadziioannou G. Polymer 1998;39:6429.
[12] Storey RF, Shoemake KA, Mays JW, Harville S. J Polym Sci, Part A: Polym Chem 1997;35:3767.
[13] Frater DJ, Mays JW, Jackson C. J Polym Sci, Part B: Polym Phys 1997;35:141.
[14] Storey RF, Shoemake KA, Chisholm BJ. J Polym Sci, Part A: Polym Chem 1996;34:2003.
[15] Tsitsilianis C, Graff S, Rempp P. Eur Polym J 1991;27:243.
[16] I-Chen L, Tsiang RC, James W, Jin-Shang L, Hun-Chang S. J Appl Polym Sci 2002;83:1911.
[17] Tseng-Yeong W, Tsiang RC, James W, Jin-Shang L, Hun-Chang S. J Appl Polym Sci 2001;79:1838.
[18] Bravo J, Tarazona MP, Saiz E. Macromolecules 1991;24:4089.
[19] Bravo J, Tarazona MP, Saiz E. Macromolecules 1992;25:625.

[20] Bravo J, Tarazona MP, Carriedo G, Gonzalez P. Polymer 1999;40: 4251.
[21] Ishizu K, Sunahara K, Asai SI. Polymer 1998;4:953.
[22] Hoxmeier RJ. US Patent 4,879,349; 1989.
[23] Breslow DS, Matlack AS. US Patent 3,113,986; 1963.
[24] Wald MW, Quam MG. US Patent 3,595,942; 1971.
[25] Hou H, Tsiang RC, Hsieh HC. J Polym Sci, Part A: Polym Chem 1997;35:2969.
[26] Young RN, Fetters LJ. Macromolecules 1978;11:899.
[27] De Gennes PG. Scaling concepts in polymer physics. Ithaca NY: Cornell University Press; 1979.
[28] Hadjichristidis N, Lindner JS, Mays JW, Wilson WW. Macromolecules 1991;24:6725.
[29] Li J, Harville S, Mays JW. Macromolecules 1997;30:466.
[30] Bauer BJ, Fetters LJ, Graessley WW, Hadjichristidis N, Quack GF. Macromolecules 1989;22:2337.
[31] Davidson NS, Fetters LJ, Funk WG, Graessley WW, Gadjichristidis N. Macromolecules 1987;20:2614.
[32] Roovers JEL, Bywater S. Macromolecules 1972;5:384.
[33] Roovers JEL, Bywater S. Macromolecules 1974;7:443.
[34] Pyun CW, Fixman M. J Chem Phys 1964;41:937.
[35] Oono YJ. J Chem Phys 1983;79:4629.
[36] Pyun CW, Fixman M. J Chem Phys 1965;42:3838.